VERSITA

CELLULAR & MOLECULAR BIOLOGY LETTERS
http://www.cmbl.org.pl

Received: 24 June 2010
Final form accepted: 08 September 2010
Published online: 17 September 2010

Volume 15 (2010) pp 651-664
DOI: 10.2478/s11658-010-0034-0

Research article

RIBOSOMAL DNA, TRI- AND BI-PARTITE PERICENTROMERES IN THE PERMANENT TRANSLOCATION HETEROZYGOTE *Rhoeo spathacea*

HIERONIM GOLCZYK[1]*, ROBERT HASTEROK[2] and MAREK SZKLARCZYK[3]

[1]Department of Plant Cytology and Embryology, Institute of Botany, Jagiellonian University, Grodzka 52, 31-044 Kraków, Poland, [2]Department of Plant Anatomy and Cytology, University of Silesia, Jagiellońska 28, 40-032 Katowice, Poland, [3]Department of Genetics, Plant Breeding and Seed Science, Agricultural University of Krakow, Al. 29 Listopada 54, 31-425 Kraków, Poland

Abstract: High- and low-stringency FISH and base-specific fluorescence were performed on the permanent translocation heterozygote *Rhoeo spathacea* (2n = 12). Our results indicate that 45S rDNA arrays, rDNA-related sequences and other GC-rich DNA fraction(s) are located within the pericentromeric regions of all twelve chromosomes, usually colocalizing with the chromomycin A_3-positive bands. Homogenization of the pericentromeric regions appears to result from the concerted spread of GC-rich sequences, with differential amplification likely. We found new 5S rDNA patterns, which suggest a variability in the breakpoints and in the consequent chromosome reorganizations. It was found that the large 5S rDNA locus residing on each of the 8E and 9E arms consisted of two smaller loci. On each of the two chromosome arms 3b and 4b, in addition to the major subtelomeric 5S rDNA locus, a new minor locus was found interstitially about 40% along the arm length. The arrangement of cytotogenetic landmarks and chromosome arm measurements are discussed with regard to genome repatterning in *Rhoeo*.

Key words: Pericentromere, Permanent translocation heterozygosity, rDNA, *Rhoeo*

---

* Author for correspondence. e-mail: h.golczyk@wp.pl, tel./fax +48-12-4228107

Abbreviations used: CMA_3^+ – chromomycin A_3 positive; FISH – fluorescence *in situ* hybridization; NORs – nucleolus organizer regions; PTH – permanent translocation heterozygosity; rDNA – ribosomal DNA; WATs – whole arm translocations

INTRODUCTION

Permanent translocation heterozygosity (PTH) presents an excellent opportunity for studies on complex genome rearrangements [1, 2]. It involves non-homologous chromosomes and results in ring/chain formation during meiosis in PTH organisms. PTH individuals breed true for meiotic multiples thanks to the existence of the two non-recombining super linkage chromosome sets called Renner complexes [1, 3-5], coupled with selection against homozygotes [6]. *Rhoeo spathacea* (Sw.) Stearn (synon. *Tradescantia spathacea*, Commelinaceae) is a textbook example of a PTH organism. It has large and non-uniform chromosomes, making it a favourable model organism for chromosome research [7]. The basic features of its karyotype, including chromosome morphology [3, 7, 8], and the distribution of heterochromatin [9-11], NORs and 5S rRNA genes [3, 12-13] have already been well characterized, and a FISH-based system for the identification of each chromosome arm has been developed [3].

The model proposed for chromosome rearrangements in *R. spathacea* favours breakpoints within or near prominent blocks of centromeric heterochromatin, based on the absence of interstitial heterochromatin and the overall length similarities of the chromosome arms seen conjoining during diakinesis [3]. Our recent results support this hypothesis [14]. We demonstrated that chromomycin A_3-positive (CMA_3^+) bands could briefly be detected not only within some NOR-related chromosome ends but also within the pericentromeric regions, which lacked detectable 45S rDNA sites and showed no obvious NOR activity. We suggested that GC-rich domains may have served as sites of interchromosomal whole-arm exchanges facilitating the spreading of the centromere-adjacent sequences and the homogenization of the pericentromeres [14]. The origin and nature of the GC-rich pericentromeric chromatin in *R. spathacea* remain unknown. Here, based on rDNA-FISH and base-specific fluorescence, we found 45S rDNA within all twelve pericentromeres and precisely mapped GC-rich pericentromeric bands in relation to the AT-rich genome fraction. We propose that these bands could be derived from subtelomeric 45S rDNA. We also present for the first time new 5S rDNA patterns on chromosomes 3, 4, 9 and 8 and the complete standard karyotype, which is based on chromosome arm measurements and the mapped cytogenetic landmarks. The possible mechanisms responsible for the arrangement of the rDNA and other GC-rich DNA fractions are discussed.

MATERIALS AND METHODS

Plant material

Three previously described [3] *R. spathacea* accessions were grown in the greenhouse at 25-28ºC. Young flower buds ca. 2 to 4 mm in length were isolated from the inflorescences and fixed in 3:1 ethanol-glacial acetic acid. For the study on the mitotic chromosomes, plant cuttings were grown in tap water to induce adventitious roots. The young roots were then excised, pre-treated with

a saturated solution of α-bromonaphtalene for 2 h, and fixed in 3:1 ethanol-glacial acetic acid.

Chromosome preparation

Dissected anthers or enzymatically digested root tips were squashed in a drop of 45% acetic acid, as described previously [3] After squashing and freezing using the dry-ice method, the cover slips were removed and the preparations were air-dried. Additional steps were taken to obtain cytoplasm-free chromosome spreads for FISH as compared to the previous study [3]. Selected preparations were treated with 0.1% pepsin solution in 0.01 N HCl for 25 min at 37ºC, washed several times in 2 × SSC and dried through an ethanol series prior to FISH.

Base-specific fluorescence

To reveal the GC- or AT-rich chromosome sites, root tip preparations were stained with 4'-6-diamidino-2-phenyloindole (DAPI) or chromomycin A_3 (CMA_3) and respectively counterstained with actinomycin D (AMD) or distamycin A (DA), as described by Schweizer and Ambros [15]. After the washing and drying, the preparations were sealed with rubber cement (Marabu). Six metaphases from each accession were selected for the detailed mapping of the AT- and GC-rich chromosome regions.

Fluorescence *in situ* hybridization (FISH)

FISH was carried out directly on freshly made, cytoplasm-free preparations or sequentially on fluorochrome-stained preparations in each clone. After removing the coverslips, the fluorochrome-stained preparations were destained in fresh 3:1 ethanol-glacial acetic acid for 30 min, washed for 30 min in absolute ethanol, and then air-dried. The two probes used for *in situ* hybridization were the 2.3-kb *Cla*I fragment of the 25S rDNA ribosomal gene of *A. thaliana* [16] and the 410-bp 5S rDNA wheat clone pTa794 [17]. Nick translation labelling of the cloned 25S rDNA fragment yielded a 70- to 150-bp electrophoretic smear. The other details of the labelling and the standard high-stringency FISH protocol were as described by Jenkins and Hasterok [18]. Additionally, a modified protocol was applied to check if the 25S rDNA-FISH foci can be detected within mitotic pericentromeres at low stringency. The two parameters were changed in relation to the standard FISH protocol: the temperature of all the post-hybridisation washes was 37ºC and the concentration of SSC in the formamide-containing wash solution was 0.4×. Freshly made high-quality mitotic preparations from each accession were subjected directly to such low-stringency FISH (Fig. 1D). Afterward, some of the preparations were reprobed with 5S rDNA at high stringency (Fig. 1E).

Image recording and processing, chromosome measurements and calculations

The pictures were taken using Nikon Eclipse 80i and Zeiss Axioplan microscopes equipped with cooled monochrome CCD cameras. CMA_3^+ signals were visualized with the aid of a narrow band (430-440 nm) excitation filter.

The digital tinting, superimposing and uniform image processing of the FISH-images were carried out using Adobe Photoshop CS3 software. For the chromosome arm measurements and karyogram construction, eighteen mitotic metaphases (six chromosome complements from each accession) subjected to a sequential DAPI/AMD-FISH procedure were analyzed. Chromosome identification was done according to the rules described previously [3]. The identified chromosome arms were designated using a combination of numbers [3] and letters [7, 8], as shown on Fig. 3 and Tab. 2. Chromosome measurements on digitally captured metaphases were performed with UTHSCSA ImageTool v.3.0 [19]. To avoid large deviations caused by different degrees of chromatin condensation between the studied metaphases, chromosome lengths were expressed as percentages of the total karyotype length (expressed as 100%). Statistical calculations and averaging were conducted using Microsoft Office Excel 2003.

RESULTS

The distribution of rDNA hybridization sites and GC- and AT-rich chromatin domains

The twelve meiotic chromosomes repeatedly showed the presence of low amounts of pericentromeric 25S rDNA at high stringency, although sometimes not all of the rDNA-FISH signals were visible at the same time within a given meiotic multiple (Fig. 1A). DAPI-positive collective chromocenters in meiotic nuclei also displayed weak 25S rDNA hybridization foci (Fig. 1B, C). The same FISH conditions produced no obvious pericentromeric 25S rDNA signals during mitosis, but after decreasing the stringency, the pericentromeric 25S rDNA hybridization signals were clearly visible on all of the mitotic chromosomes (Figs 1D, 2). The distribution and size of the distal 45S rDNA loci after modified (Figs 1D, 2) and standard FISH (Fig. 1G) were the same, and closely matched the pattern previously described [3]. Important differences can be distinguished between submetacentric chromosome "pairs" (chromosomes: 2-3, 5-6, 8-9) with regard to the size of distal 45S rDNA loci localized on their short arms.

Judging by the size and intensity of the hybridization signals, there seems to be a gradient of rDNA copy number, with chromosomes 8 and 9 having the highest rDNA copy number, chromosomes 2 and 3 also having a high rDNA amount, but lower than that of 8 and 9, and chromosomes 5-6 clearly having the smallest rDNA array (Figs 1D, 1G, 2). This trend in rDNA amount correlates with the size differences between the corresponding CMA_3^+ bands (Figs 1F, 1I, 2). The transcriptionally active 45S rDNA loci on chromosomes 5, 6, 10, and 11 [3] are much smaller than those on chromosomes 2, 3, 8 and 9, and are hardly if at all detectable using CMA_3 fluorescence (Figs 1F, 1I, 2). This finding confirms a general correlation between the amount of subtelomeric 45S rDNA and the GC

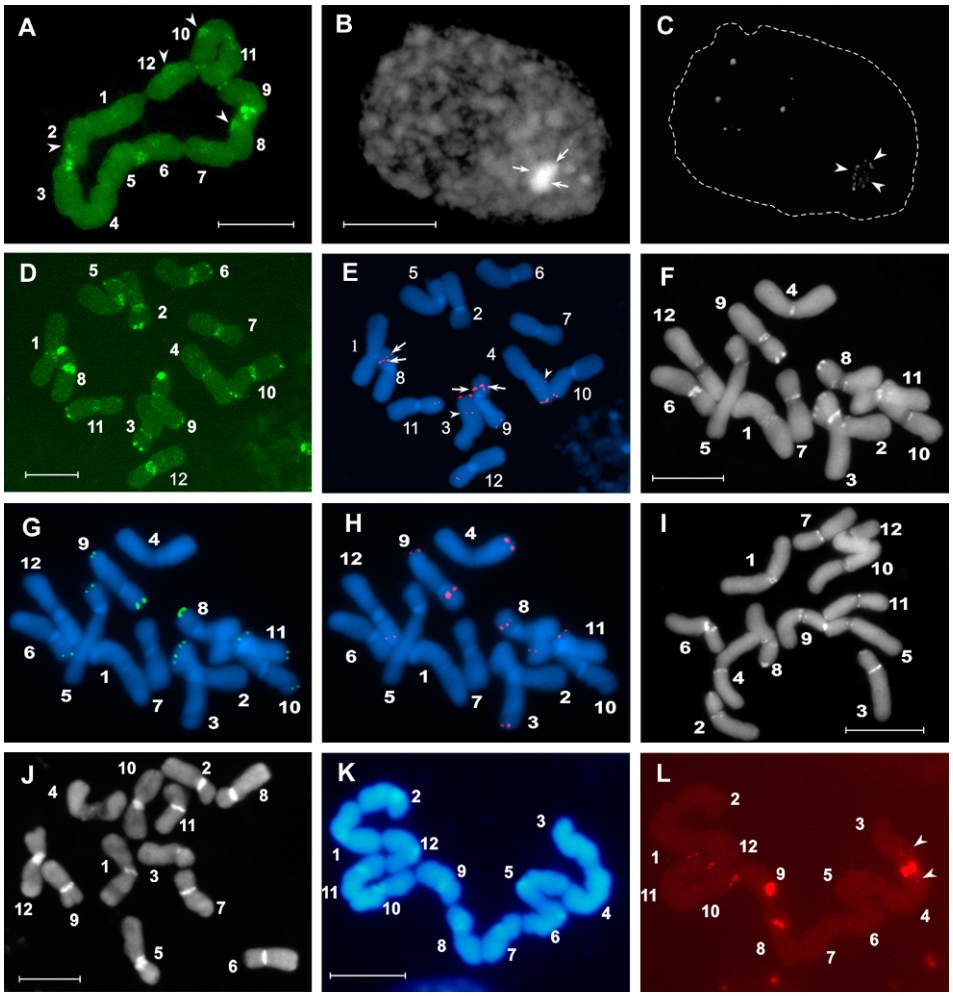

Fig. 1. Chromosomes of *Rhoeo spathacea* analyzed using the FISH, CMA_3/DA-FISH and DAPI/AMD-FISH techniques. The chromosomes are numbered according to Golczyk *et al.* (2005). A, B, C – High stringency FISH with 25S rDNA (green) probe performed on a (A) meiotic ring, and (B-C) leptotene nucleus. B – DAPI image showing the large collective chromocenter; C – The same meiotic nucleus after rDNA-FISH, graphically outlined (dashed line), arrows – collective chromocenter, arrowheads – pericentromeric 25S rDNA sites. D, E – Low stringency FISH with 25S rDNA (green) (D) and high stringency FISH after reprobing of the preparation with 5S rDNA (red) (E), arrows – two subloci forming the duplicated 5S rDNA mojor locus on each of the chromosome arms 8E and 9E, arrowheads – interstitial 5S rDNA minor loci on chromosome arms 3b and 4b. F, G, H – Sequential CMA_3/DA-FISH and DAPI/AMD-FISH at high stringency. F – CMA_3/DA; G – FISH with 25S rDNA probe (green); H – FISH with 5S rDNA (red) probe; I – CMA_3/DA. J – DAPI/AMD. K, L – DAPI staining (K) and high stringency FISH with a 5S rDNA probe (L) performed on a meiotic chain, arrowheads – interstitial 5S rDNA loci on chromosome arms 3b and 4b. Scale bars = 5 μm.

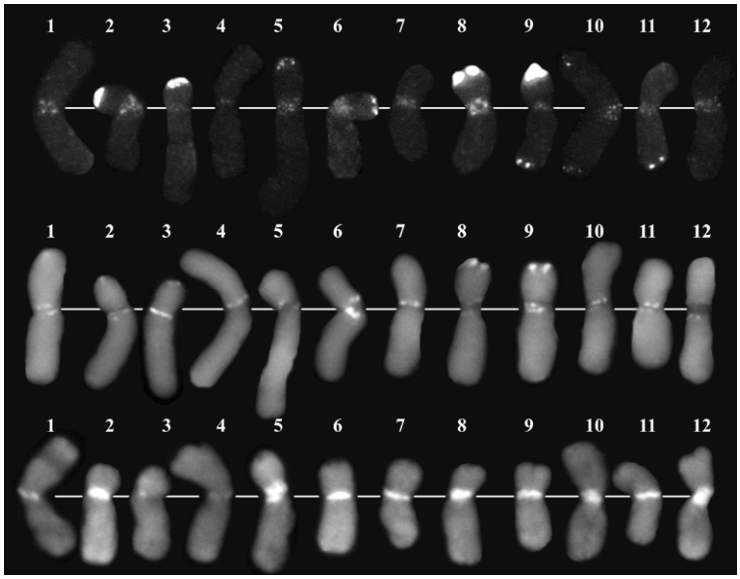

Fig. 2. Low stringency FISH with 25S rDNA, and the CMA_3/DA or DAPI/AMD techniques on somatic chromosomes of *R .spathacea*. Top row – FISH, middle row – CMA_3/DA, bottom row – AMD/DAPI.

content, and also shows the essential limit of sensitivity of CMA_3 fluorescence in detecting NORs in *R. spathacea*. This study clearly demonstrates the existence of cytologically distinct AT- and GC-rich DNA fractions (bands), forming bi- and tripartite pericentromeres in *R. spathacea*. Each compound pericentromere consists of a central AT-rich domain and one or two lateral GC-rich bands (Figs 1F, 1I, 1J, 2). All of the chromosomes but three (1, 3 and 4) possess large centromeric DAPI bands. Chromosomes 3 and 4 have only some tiny, and therefore difficult to quantify AT-rich DNA fraction around the centromere (Fig. 1J). Chromosomes 2, 5, 8, 10 and 12 have the most prominent AT-rich segments, each comprising ca. 1% of the karyotype, and chromosomes 6, 7, 9 and 11 have DAPI bands of medium size, within the range of 0.6-0.7% (Tab. 1).

Tab. 1. The mean amount of AT-rich pericentromeric heterochromatin in each of the individual chromosomes (1-12) expressed as a percentage of the karyotype length. Standard deviations within brackets; [0.00]: AT-rich segments difficult for cytological quantification.

1	2	3	4	5	6	7	8	9	10	11	12	Total
0.32	1.00			1.09	0.77	0.65	0.99	0.65	0.94	0.71	1.16	8.28
(0.10)	(0.21)	[0.00]	[0.00]	(0.30)	(0.19)	(0.22)	(0.37)	(0.17)	(0.27)	(0.18)	(0.24)	(2.15)

In total, the AT-rich pericentromeric chromatin constitutes ca. 8% of the genome (Tab. 1). The GC-rich chromosome segments flanking the AT-centromere band on both sides are consistently found on chromosomes 1, 5, 6, 8, 9, 11 and 12,

whereas chromosomes 2, 3, 4, 7 and 10 have only one reproducible pericentromeric GC-band, respectively localized within the proximal region of arms 2a, 3b, 4C, 7D and 10F (Figs 1F, 1I, 2, 3). 25S rDNA hybridization sites under low stringency conditions colocalize with GC-rich bands on all of the chromosomes, but minute rDNA hybridization signals are also dispersed throughout the pericentromeres (Figs 1D, 2).

The pericentromeric regions do not maintain the correlation between the size of the 25S rDNA hybridisation signals and the intensity of the CMA_3 fluorescence found at the NORs. The pericentromeric 25S rDNA hybridization sites (low stringency), although generally much smaller than the distal ones of chromosomes 2 and 3, colocalized with clearly visible, stable CMA_3^+ bands (Figs 1D, 1F, 1I, 2). A striking example is chromosome 6, which has a pericentromeric CMA_3^+ band comparable or even larger than the one associated with the NORs on chromosomes 8 and 9 (Figs 1F, 1I, 2).

New 5S rDNA arrangements were revealed. The major 5S rDNA loci residing on arms 8E and 9E appeared to be bipartite, actually consisting of two closely linked smaller subloci (Fig. 1E). The double nature of these loci was not always seen on meiotic chromosomes or within sequentially analysed mitotic preparations (Fig. 1H, K-L), but was detected repeatedly in each eccession, at both high and low stringency, when freshly made high-quality mitotic preparations were subjected directly to FISH. Furthermore, on each of the 4b and 3b chromosome arms, a new minor interstitial 5S rDNA locus was found in addition to the major subtelomeric site, at a position corresponding to ca. 40% of the arm length (Fig. 1E, K-L). These two 5S rDNA loci as a rule were revealed as stringency-independent hybridization sites within freshly made meiotic and mitotic preparations, but were sometimes barely detected on sequentially treated chromosomes.

Standard *R. spathacea* karyotype – are the homologous chromosome arms perfectly matched in length?

Double-target FISH was used to unequivocally identify each chromosome arm, and it allowed exact measurements, which are shown here for the first time (Tab. 2). Student's test was used to estimate significant mismatches in length within each of the twelve chromosome arm pairs (1a-2a, 2B-3B, 3b-4b, 4C-5C, 5c-6c, 6D-7D, 7d-8d, 8E-9E, 9e-10e, 10F-11F, 11f-12f, 12A-1A), with a null hypothesis that any two homologous arms were the same in length. The null hypothesis could be accepted ($P > 0.05$) for six positions: 2B-3B, 3b-4b, 5c-6c, 8E-9E, 10F-11F and 11f-12f. The rest of the homologous arms (1a-2a, 4C-5C, 6D-7D, 7d-8d, 9e-10e and 12A-1A) appear not to be identical in length ($P < 0.05$), as shown in Tab. 3. At two positions, 4C-5C and 6D-7D, the arms are vastly unequal in length (Fig. 3, Tabs 2, 3). Each of the two imperfect length matches accounts for ca. 1.7% length difference, which is roughly equivalent to 1/4 of the 5C arm and to 1/3 of the 6D arm (Fig. 3, Tab. 3).

Tab. 2. The mean lengths of the chromosomes and their arms, and the chromosome morphology in the ring-forming *R. spathacea*. Standard deviations within brackets. 1-12, individual chromosomes; 1A-12A, individual chromosome arms; I, chromosome arm length; II, chromosome length; III, arm ratio; IV, chromosome morphology, m – metacentric (arm ratio = 1-1.7), sm – submetacentric (arm ratio = 1.7-3.0).

		I	II	III	IV
1	1A	5.40 (036)	9.88 (0.51)	1.21 (0.14)	m
	1a	4.48 (0.33)			
2	2a	5.34 (0.35)	7.77 (0.38)	2.20 (0.38)	sm
	2B	2.43 (0.30)			
3	3B	2.31(0.35)	8.12 (0.62)	2.52 (0.44)	sm
	3b	5.81 (0.46)			
4	4b	5.25 (0.45)	10.04 (0.64)	1.10 (0.08)	m
	4C	4.79 (0.31)			
5	5C	6.46 (0.97)	9.22 (0.71)	2,34 (0.40)	sm
	5c	2.76 (0.72)			
6	6c	2.77 (0.56)	7.59 (0.56)	1.74 (0.27)	sm
	6D	4.82 (0.53)			
7	7D	3.03 (0.25)	7.46 (0.39)	1.46 (0.14)	m
	7d	4.43 (0.26)			
8	8d	4.98 (0.38)	7.83 (0.61)	1.75 (0.24)	sm
	8E	2.85 (0.37)			
9	9E	2.48 (0.38)	7.46 (0.66)	2.01 (0.40)	sm
	9e	4.98 (0.45)			
10	10e	4.42 (0.38)	8.80 (0.73)	1.01 (0.09)	m
	10F	4.38 (0.52)			
11	11F	4.22 (0.28)	7.61 (0.43)	1.24 (0.13)	m
	11f	3.39 (0.29)			
12	12f	3.43 (0.33)	8.22 (0.64)	1.40 (0.16)	m
	12A	4.79 (0.48)			

Tab. 3. Statistically significant length differences (Student's test, $P < 0.05$) between homologous chromosome arms in *R. spathacea*. A.P., arm position. Standard deviations within brackets.

A.P	1a – 2a	4C – 5C	6D – 7D	7d – 8d	9e – 10e	12A – 1A	Total
	0.86	1.67	1.79	0.55	0.56	0.61	6.10
	(0.37)	(0.49)	(0.43)	(0.29)	(0.32)	(0.25)	(2.01)

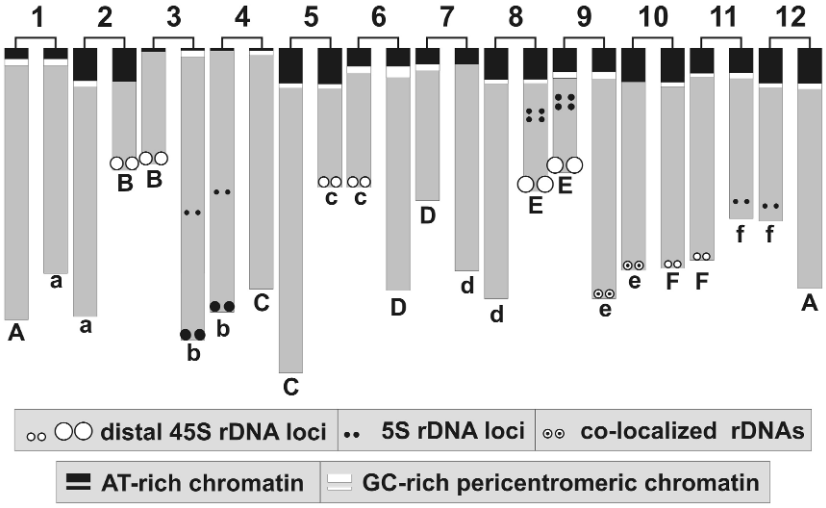

Fig. 3. A karyogram showing the measured chromosomes (1-12) arranged in meiotic order. The chromosomes are bent to demonstrate the arm length relationships. The regions depicting the AT-rich and GC-rich pericentromeric chromatin are not drawn to scale.

DISCUSSION

Permanent translocation heterozygosity is known to occur in at least fifty-seven species of flowering plants [2]. There is also recent evidence suggesting its existence in vertebrates, in two Discus fish species where meiotic chains comprising as many as 20 chromosomes were repeatedly found in both sexes [20]. The fact that this unusual genetic syndrome has evolved in diverse unrelated taxa indicates that, in spite of the apparent disadvantages (e.g. restricted recombination resulting in a clonal reproduction, complicated and erroneous meiotic segregation), it may serve as a fully successful alternative strategy in adaptive evolution, during which karyotype structure seems to be one of the main features subjected to selection [1]. Unfortunately, the cyto-molecular constitution of Renner complexes is still poorly understood in the majority of known PTH organisms. It seems that the length of the translocated chromosome segments largely depends on the distribution of heterochromatin, which by accumulating satellite DNA and transposable elements, may be a preferable site for breakages [21, 22]. Exchanges of diverse, often distal portions of chromosome arms are postulated in *Gibasis pulchella*, where C-banding is mainly intercalary [23] and in the two Discus fish species where heterochromatin not only resides at the pericentromeres but also constitutes a large proximal portion of some of the chromosome arms [20, 24]. Whole arm translocations (WATs) are postulated to have operated in *Oenothera* and *R. spathacea*. In both taxa, heterochromatic blocks around the centromeres and overall length similarities of the chromosome arms conjoining during diakinesis are evident [1, 3, 4].

The 25S rDNA hybridization signals seen here at both low and high stringency may suggest that whole-arm exchanges were accompanied or preceded by whole-arm inversions. A paracentric inversion through the simultaneous incidence of breaks within a subtelomeric NOR and in the pericentromere itself could have been a possible mechanism seeding rRNA genes into the pericentromeric area. Parts of a large rDNA array shifted from the subtelomeric region to the pericentromere by paracentric inversion may then have invaded the other side of the centromere and other pericentromeres through pericentric inversion and WATs, i.e. an ectopic exchange between non-homologous pericentromeres. Of the chromosome breakpoints contributing to evolutionary karyotype repatterning in *Arabidopsis*, about 85% were found close to centromeres or chromosome termini [22]. In the genus *Tradescantia*, which now contains *R. spathacea* [25], inversions seem to be widespread [26-28]. In *R. spathacea*, pericentromeric regions of all of the chromosomes have a strong tendency for ectopic pairing in meiotic and somatic cells [3, 9, 29], which could be a framework for the WAT-generated spread of their sequences and the resultant perientromere homogenization by GC-rich sequences [discussed in 14].

Ribosomal DNA is frequently involved in karyotype remodelling [30-34]. Its potential for rearrangements was sometimes explained by its fragility [35]. Hall and Parker [32] hypothesized that the NOR itself when transferred to the centromeric region could cause chromosomal instability resulting in chromosomal fission. If breakpoints occurred preferentially adjacent to AT-rich centromeric heterochromatin, AT-rich and GC-rich sequences would be intermixed to some extent, but they also should form distinct islands. Our statistical analysis indicates that not all of the homologous chromosome arms are the same in length. The differences concerning four arm positions (1a-2a, 7d-8d, 9e-10e, 12A-1A), although significant, are relatively minor, but those of the two remaining positions (4C-5C, 6D-7D) are striking (Fig. 3). The length dissimilarity between any two conjugating arms in a PTH organism can result from unequal reciprocal translocations with differently localized breakpoints. However, considering WATs, the difference may indicate deletion, duplication or even a more complex scenario, e.g. pericentric inversion changing the morphology of one of the chromosomes involved, followed later by WAT. Half of the homologous arms are perfectly matched in length (2B-3B, 3b-4b, 5c-6c, 8E-9E, 10F-11F, 11f-12f); thus, the involvement of the chromosomes harbouring them in whole arm rearrangements seems conceivable.

In general, models of karyotype evolution are becoming more complex than previously envisaged, as combinations of peri- and/or paracentric inversions and translocations are now thought to be frequent [22, 24, 36, 37]. In both animals and plants, structural rearrangements are among the mechanisms proposed to be involved in relocating rDNA or seeding its parts (if a breakpoint splits a locus into minor ones), creating new rDNA loci [38-41].

The failure to detect pericentromeric rDNA sites on mitotic chromosomes at high stringency and rDNA-FISH signals within meiotic pericentromeres may be

related to chromatin condensation. Within the more compacted meiotic chromatin, short and dispersed rDNA arrays are more likely to be brought into closer proximity, thus increasing local signal intensity. A similar enhancement of the FISH signals in meiotic chromatin was also noted in Discus fish [42]. The low stringency rDNA hybridization signals at the mitotic pericentromeres are likely to reflect the presence of pericentromeric rDNA-derived sequences, possibly degenerate ones (see the Materials and Methods section). We have shown that in some chromosomes rDNA-FISH in low stringency experiments at pericentromeric regions does not correspond to the size of colocalizing CMA_3^+ bands. This contrasts with what was observed for NORs (see Fig. 2). Pericentromeric CMA_3^+ bands on many chromosomes proved to be stable, and substantially larger/brighter than the NOR CMA_3^+ regions on chromosomes 2 and 3 (Fig. 2). This indicates that pericentromeric CMA_3^+ bands also contain some other type of GC-rich DNA, possibly satellite sequences, and that pericentromere homogenization in *R. spathacea* was based not only on the concerted spread of GC-rich sequences, but also included their differential amplification. The newly discovered 5S rDNA pattern may suggest some variability of breakpoints and the consequent chromosome reorganisation. The duplicated 5S rDNA locus on arms 8E and 9E (Figs 1E, 3) may have been the result of a small paracentric inversion with one of the breakpoints within the existing major 5S rDNA locus. In adition, each of the two interstitial minor 5S rDNA loci on chromosome arms 3b and 4b (Figs 1E, 1L, 3) could have resulted from a large segmental inversion, involving ca. 40% of the arm length, with one of the breakpoints within the subtelomeric major 5S rDNA locus (Fig. 3). As the two proposed inversions are homozygous, this would indicate their ancient occurrence, prior to translocations.

Translocations and/or inversions are frequently ascribed to the misrepair of double strand breaks by ectopic recombination, i.e. homologous recombination between tandemly repeated DNA sequences or transposable elements, which could serve as sites for chromosome exchange [43]. An alternative type of rDNA mobility which could be involved in the arrangement of the described cytogenetic landmarks in *R. spathacea* may be rDNA movement without altering linkage groups, suggested by Dubcovsky & Dvořák [44], and also by Schubert & Wobus [30], who proposed that NORs may jump within and between chromosomes via the dispersion and magnification of minor loci consisting of a few rDNA copies. Ribosomal DNA transposition and/or the involvement of mobile elements are frequently proposed mechanisms explaining such a mode of rDNA dispersion (reviewed in [45]). Further studies are needed to evaluate a real means of spreading the initial as well as the modified (e.g. degenerate, amplified) GC-rich DNA sequences like rDNA or other GC-rich DNA fractions in a highly organized fashion, which seems important for shaping the bi- and tripartite pericentromeres in *R. spathacea.*

Acknowledgements. The study was funded by grant N301 116 32/4008 from the Polish Ministry of Science and Higher Education. The authors would like to thank Dr. Tim Langdon (IBERS, Aberystwyth University, UK) for his valuable comments on the manuscript.

REFERENCES

1. Cleland, R.E. ***Oenothera*. Cytogenetics and evolution**, Academic Press, London and New York, 1972.
2. Holsinger, K.E. and Ellstrand, N.C. The evolution and ecology of permanent translocation heterozygotes. **Am. Nat.** 124 (1984) 48-71.
3. Golczyk, H., Hasterok, R. and Joachimiak, A.J. FISH-aimed karyotyping and characterization of Renner complexes in permanent heterozygote *Rhoeo spathacea*. **Genome** 48 (2005) 145-153.
4. Golczyk, H., Musial, K., Rauwolf, U., Meurer, J., Herrmann, R.G. and Greiner, S. Meiotic events in *Oenothera* - a non-standard pattern of chromosome behaviour. **Genome** 51 (2008) 952-958.
5. Rauwolf, U., Golczyk, H., Meurer, J., Herrmann, R.G. and Greiner, S. Molecular marker systems for *Oenothera* genetics. **Genetics** 180 (2008) 1289-1306.
6. Levin, D.A. **The role of chromosomal change in plant evolution**, Oxford University Press, New York, 2002.
7. Sax, K. Chromosome ring formation in *Rhoeo discolor*. **Cytologia** 3 (1931) 36-53.
8. Lin, Y.J. and Paddock, E.F. Ring-position and frequency of adjacent distribution of meiotic chromosomes in *Rhoeo spathacea*. **Am. J. Bot.** 60 (1973) 685-690.
9. Natarajan, A.T. and Natarajan, S. The heterochromatin of *Rhoeo discolor*. **Hereditas** 72 (1972) 323-330.
10. Pettenati, M.J. Giemsa C-banding of *Rhoeo* (*Commelinaceae*). **Genetica** 74 (1987) 219-224.
11. Golczyk, H. and Joachimiak, A. Karyotype structure and interphase chromatin organization in *Rhoeo spathacea* (Sw.) Stearn (*Commelinaceae*). **Acta Biol. Cracov. Ser. Bot.** 41 (1999) 143-150.
12. Carniel, K. Enständige nucleolen und zahl der nucleolenchromosomen bei *Rhoeo discolor*. **Öster. Bot. Z.** 107 (1960) 403-408.
13. Golczyk, H. and Joachimiak, A. NORs in *Rhoeo* revisited. **Caryologia** 56 (2003) 31-35.
14. Golczyk, H., Joachimiak, A. and Hasterok, R. Pericentromeric GC-rich chromatin in *Rhoeo*. Evidence from soma and germ-line. **Caryologia** 61 (2008) 388-391.
15. Schweizer, D. and Ambros, P.F. Chromosome banding. **Meth. Mol. Biol.** 29 (1994) 97-111.

16. Unfried, I. and Gruendler, P. Nucleotide sequence of the 5.8S and 25S rRNA genes and the internal transcribed spacers from *Arabidopsis thaliana*. **Nucleic Acids Res.** 18 (1990) 4011.
17. Gerlach, W.L. and Dyer, T.A. Sequence organization of the repeating units in the nucleus of wheat which contain 5S rRNA genes. **Nucleic Acids Res.** 11 (1980) 4851-4865.
18. Jenkins, G. and Hasterok, R. BAC landing on chromosomes of *Brachypodium distachyon* for comparative genome alignment. **Nat. Protoc.** 2 (2007) 88-98.
19. UTHSCSA ImageTool v.3.0 (http://ddsdx.uthscsa.edu/dig/itdesc.html).
20. Gross, M.C., Feldberg, E., Cella, D.M., Schneider, M.C., Schneider, C.H., Porto, J.I.R. and Martins, C. Intriguing evidence of translocations in Discus fish (*Symphysodon*, *Cichlidae*) and a report of the largest meiotic chromosomal chain observed in vertebrates. **Heredity** 102 (2009) 435-441.
21. Bennetzen, J.L. Transposable element contributions to plant gene and genome evolution. **Plant Mol. Biol.** 42 (2000) 251-269.
22. Schubert, I. Chromosome evolution. **Curr. Opin. Plant Biol.** 10 (2007) 109-115.
23. Kenton, A., Davies, A. and Jones, K, Identification of Renner complexes and duplications in permanent hybrids of *Gibasis pulchella* (*Commelinaceae*). **Chromosoma** 95 (1987) 424-434.
24. Mesquita, D.R., Porto, J.I.R. and Feldberg, E. Chromosomal variability in the wild ornamental species of *Symphysodon* (*Perciformes: Cichlidae*) from Amazon. **Neotrop. Ichthyol.** 6 (2008) 181-190.
25. Hunt, D.R. *Campelia*, *Rhoeo*, *Zebrina* united with *Tradescantia*. **Kew Bull.** 41 (1986) 401-405.
26. Darlington, C.D. Chromosome behaviour and structural hybridity in the *Tradescantiae*. II. **Jour. Genet.** 35 (1937) 259-280.
27. Sax, K. Chromosome behaviour and nuclear development in *Tradescantia*. **Genetics** 22 (1937) 523-533.
28. Swanson, C.R. The distribution of inversions in *Tradescantia*. **Genetics** 25 (1940) 438-465.
29. Coleman, L.C. The relation of chromocentres to the differential segments in *Rhoeo discolor* Hance. **Amer. J. Bot.** 28 (1941) 742-748.
30. Schubert, I. and Wobus, U. In situ hybridization confirms jumping nucleolus organizing regions in *Allium*. Chromosoma 92 (1985) 143-148.
31. Cheung, S.W., Sun, L. and Featherstone, T. Molecular cytogenetic evidence to characterize breakpoint regions in Robertsonian translocations. **Cytogenet. Cell Genet.** 54 (1990) 97-102.
32. Hall, K.J. and Parker, J.S. Stable chromosome fission associated with rDNA mobility. **Chromosome Res.** 3 (1995) 417-422.
33. Thomas, H.M., Harper, J.A. and Morgan, W.G. Gross chromosome rearrangements are occurring in an accession of the grass *Lolium rigidum*. **Chromosome Res.** 9 (2001) 585-590.

34. Gernand, D., Golczyk, H., Rutten, T., Ilnicki, T., Houben, A. and Joachimiak, A.J. Tissue culture triggers chromosome alterations, amplification and transposition of repeat sequences in *Allium fistulosum*. **Genome** 50 (2007) 435-442.
35. Butler, D.K. Ribosomal DNA is a site of chromosome breakage in aneuploid strains of *Neurospora*. **Genetics** 131 (1992) 581-592.
36. Tagashira, N. and Kondo, K. Chromosome phylogeny of *Zamia* and *Ceratozamia* by means of Robertsonian changes detected by fluorescence *in situ* hybridization (FISH) technique of rDNA. **Plant Syst. Evol.** 227 (2001) 145-155.
37. Moscone, E.A., Samuel, R., Schwarzacher, T., Schweizer, D. and Pedrosa-Harand, A. Complex rearrangements are involved in *Cephalanthera* (*Orchidaceae*) chromosome evolution. **Chromosome Res.** 15 (2007) 931-943.
38. Hirai, H., Yamamoto, M.T., Taylor, R.W. and Imai, H.T. Genomic dispersion of 28S rDNA during karyotype evolution in the ant genus *Myrmecia* (*Formicidae*). **Chromosoma** 105 (1996) 190-196.
39. Bombarová, M., Marec, F., Nguyen, P. and Špakulová, M. Divergent location of ribosomal genes in chromosomes of fish thornyheaded worms, *Pomphorhynchus laevis* and *Pomphorhynchus tereticollis* (*Acanthocephala*). **Genetica** 131 (2007) 141-149.
40. Chung, M.C., Lee, Y.I., Cheng, Y,Y,, Chou, Y.J. and Lu, C.F. Chromosomal polymorphism of ribosomal genes in the genus *Oryza*. **Theor. Appl. Genet.** 116 (2008) 745-753.
41. Nguyen, P., Sahara, K., Yoshido, A. and Marec, F. Evolutionary dynamics of rDNA clusters on chromosomes of moths and butterflies (*Lepidoptera*). **Genetica** 138 (2010) 343-354.
42. Gross, M.C., Schneider, C.H., Valente, G.T., Porto, J.I.R., Martins, C. and Feldberg, E. Comparative cytogenetic analysis of the genus *Symphysodon* (Discus Fishes, *Cichlidae*): chromosomal characteristics of retrotransposons and minor ribosomal DNA. **Cytogenet. Genome Res.** 127 (2009) 43-53.
43. Mieczkowski, P.A., Lemoine, F.J. and Petes, T.D. Recombination between retrotransposons as a source of chromosome rearrangements in the yeast *Saccharomyces cerevisiae*. **DNA Repair** 5 (2006) 1010-1020.
44. Dubcovsky, J. and Dvořák, J. Ribosomal RNA multigene loci - nomads of the *Triticeae* genomes. **Genetics** 140 (1995) 1367-1377.
45. Cabrero, J. and Camacho, J.P.M. Location and expression of ribosomal RNA genes in grasshoppers: abundance of silent and cryptic loci. **Chromosome Res.** 16 (2008) 595-607.